Lattice determination of light quark masses

M. Göckeler,[1] R. Horsley,[2] H. Oelrich,[3] D. Petters,[3,4] D. Pleiter,[3,4] P. E. L. Rakow,[1] G. Schierholz,[3,5] and P. Stephenson[6]
[1]*Institut für Theoretische Physik, Universität Regensburg, D-93040 Regensburg, Germany*
[2]*Institut für Physik, Humboldt-Universität zu Berlin, D-10115 Berlin, Germany*
[3]*Deutsches Elektronen-Synchrotron DESY, John von Neumann-Institut für Computing NIC, D-15735 Zeuthen, Germany*
[4]*Institut für Theoretische Physik, Freie Universität Berlin, D-14195 Berlin, Germany*
[5]*Deutsches Elektronen-Synchrotron DESY, D-22603 Hamburg, Germany*
[6]*Dipartimento di Fisica, Università degli Studi di Pisa & INFN, Sezione di Pisa, I-56100 Pisa, Italy*
(Received 6 August 1999; published 27 July 2000)

A fully nonperturbative lattice determination of the up or down and strange quark masses is given for quenched QCD using both $O(a)$ improved Wilson fermions and ordinary Wilson fermions. For the strange quark mass with $O(a)$ improved fermions we obtain $m_s^{\overline{MS}}(\mu=2\ \mathrm{GeV})=105(4)$ MeV, using the interquark force scale r_0. Because of quenching problems, fits are only possible for quark masses larger than the strange quark mass. If we extrapolate our fits to the up or down quark mass we find for the average mass $m_l^{\overline{MS}}(\mu=2\ \mathrm{GeV})=4.4(2)$ MeV.

PACS number(s): 12.38.Gc, 11.15.Ha

I. INTRODUCTION

Some of the least known parameters in the standard model are the light quark masses m_u, m_d, and m_s. Their phenomenological values have been discussed since the early days of the quark model. Paradoxically, the values of the later discovered heavier quarks are more accurately known [1]. The reason is that the connection between light quark masses and observables is highly nonperturbative. This means that the lattice approach is an appropriate technique for this problem.

In this paper we shall present a completely nonperturbative determination of light quark masses. A recent major step forward has been the nonperturbative lattice determination of the renormalization constants of the mass operators. Also, because of the increase in available computer time, a more reliable continuum extrapolation is now possible.

This paper is organized as follows. In Sec. II we discuss the definition of the quark mass and its renormalization group behavior. Transcribing lattice data to physical units requires a scale to be set. For quenched QCD this problem is discussed in Sec. III. The lattice technique for obtaining the quark masses and their renormalization is presented in Sec. IV. In Sec. V we give our results, and in Sec. VI we extrapolate them to the continuum limit to remove residual discretization effects. We perform the calculations for both, $O(a)$ improved fermions and for Wilson fermions. Both should extrapolate to the same continuum result, and thus we have a consistency check between the two methods. We have previously used tadpole improved perturbation theory to compute the renormalization constants. In Sec. VII we test the validity of this approach. Finally, in Sec. VIII we give our conclusions.

II. DEFINING THE QUARK MASS

Due to confinement quarks are not eigenstates of the QCD Hamiltonian and are thus not directly observable. A definition of the quark mass from an experiment thus means prescribing the measurement procedure. Theoretically this is equivalent to giving a renormalization scheme $\mathcal{S}$ and scale M. Conventionally, quark masses are given in a mass independent scheme, such as the modified minimal subtraction ($\overline{\mathrm{MS}}$) scheme, at some given scale μ, commonly taken as 2 GeV [1]. In a general mass independent scheme $\mathcal{S}$ the renormalized quark mass is given by

$$m^{\mathcal{S}}(M)=Z_m^{\mathcal{S}}(M)m_{bare}. \tag{1}$$

The running of this renormalized quark mass as the scale M is changed is controlled by the β and γ functions in the renormalization group equation. These are defined as scale derivatives of the renormalized coupling and mass renormalization constant as

$$\beta^{\mathcal{S}}(g^{\mathcal{S}}(M))\equiv\left.\frac{\partial g^{\mathcal{S}}(M)}{\partial\log M}\right|_{bare}, \tag{2}$$

$$\gamma_m^{\mathcal{S}}(g^{\mathcal{S}}(M))\equiv\left.\frac{\partial\log Z_m^{\mathcal{S}}(M)}{\partial\log M}\right|_{bare}, \tag{3}$$

where the bare parameters are held constant. These functions are given perturbatively as power series expansions in the coupling constant. The expansion is now known to four loops in the $\overline{\mathrm{MS}}$ scheme [2,3]. We have

$$\begin{aligned}\beta^{\overline{MS}}(g)&=-b_0g^3-b_1g^5-b_2^{\overline{MS}}g^7-b_3^{\overline{MS}}g^9-\cdots,\\ \gamma_m^{\overline{MS}}(g)&=d_{m0}g^2+d_{m1}^{\overline{MS}}g^4+d_{m2}^{\overline{MS}}g^6+d_{m3}^{\overline{MS}}g^8+\cdots,\end{aligned} \tag{4}$$

where (for quenched QCD)

$$b_0=\frac{11}{(4\pi)^2},\quad b_1=\frac{102}{(4\pi)^4},$$

$$b_2^{\overline{MS}}=\frac{1}{(4\pi)^6}\left[\frac{2857}{2}\right],$$

$$b_3^{\overline{MS}}=\frac{1}{(4\pi)^8}\left[\frac{149753}{6}+3564\zeta_3\right], \tag{5}$$

and

$$d_{m0}=-\frac{8}{(4\pi)^2},\quad d_{m1}^{\overline{MS}}=-\frac{1}{(4\pi)^4}\frac{404}{3},$$

$$d_{m2}^{\overline{MS}}=-\frac{2498}{(4\pi)^6},$$

$$d_{m3}^{\overline{MS}}=-\frac{1}{(4\pi)^8}\left[\frac{4603055}{81}+\frac{271360}{27}\zeta_3-17600\zeta_5\right], \tag{6}$$

with $\zeta_3=1.20206\ldots$ and $\zeta_5=1.03693\ldots$, ζ being the Riemann zeta function.

We may immediately integrate Eq. (2) to obtain

$$M=\Lambda^{\mathcal{S}}[b_0 g^{\mathcal{S}}(M)^2]^{b_1/2b_0^2}\exp\left[\frac{1}{2b_0 g^{\mathcal{S}}(M)^2}\right]$$
$$\times\exp\left\{\int_0^{g^{\mathcal{S}}(M)}d\xi\left[\frac{1}{\beta^{\mathcal{S}}(\xi)}+\frac{1}{b_0\xi^3}-\frac{b_1}{b_0^2\xi}\right]\right\}. \tag{7}$$

The renormalization group invariant (RGI) quark mass is defined from the renormalized quark mass as

$$m^{RGI}\equiv\Delta Z_m^{\mathcal{S}}(M)m^{\mathcal{S}}(M)=\Delta Z_m^{\mathcal{S}}(M)Z_m^{\mathcal{S}}(M)m_{bare}, \tag{8}$$

where

$$[\Delta Z_m^{\mathcal{S}}(M)]^{-1}=[2b_0 g^{\mathcal{S}}(M)^2]^{-d_{m0}/2b_0}$$
$$\times\exp\left\{\int_0^{g^{\mathcal{S}}(M)}d\xi\left[\frac{\gamma_m^{\mathcal{S}}(\xi)}{\beta^{\mathcal{S}}(\xi)}+\frac{d_{m0}}{b_0\xi}\right]\right\}, \tag{9}$$

and the integration constant upon integrating Eq. (2) is given by $\Lambda^{\mathcal{S}}$, and similarly from Eq. (3) we have m^{RGI}. $\Lambda^{\mathcal{S}}$ and m^{RGI} are independent of the scale. Under a change of variable (scheme change or $\mathcal{S}\to\mathcal{S}'$),

$$g^{\mathcal{S}'}=G(g^{\mathcal{S}})=g^{\mathcal{S}}(1+c_1(g^{\mathcal{S}})^2+\cdots). \tag{10}$$

It can be shown that the first two coefficients of the β function, the first coefficient of the γ function and m^{RGI} are independent of the scheme, while Λ only changes as $\Lambda^{\mathcal{S}'}=\Lambda^{\mathcal{S}}\exp(c_1/b_0)$.

For the $\overline{\rm MS}$ scheme computing $[\Delta Z_m^{\overline{MS}}(\mu)]^{-1}$ involves first solving Eq. (7) for $g^{\overline{MS}}(\mu)$ and then evaluating Eq. (9). This gives Fig. 1. We expand the β and γ functions to the appropriate order and then numerically evaluate the integrals. At $\mu=2$ GeV we have $\mu/\Lambda^{\overline{MS}}\sim 8$, and it seems that already at this value we have a fast converging series in loop orders. Indeed, only going from one loop to two loops gives a significant change in $[\Delta Z_m^{\overline{MS}}(8\Lambda^{\overline{MS}})]^{-1}$ of order 7%. From two loops to three loops we have about 2%. The difference between the three-loop and four-loop results is $O(0.5\%)$. So if we are given m^{RGI}, and we wish to find the quark mass in the $\overline{\rm MS}$ scheme at a certain scale, we need only use the four-loop result from Eq. (9) or equivalently Fig. 1.

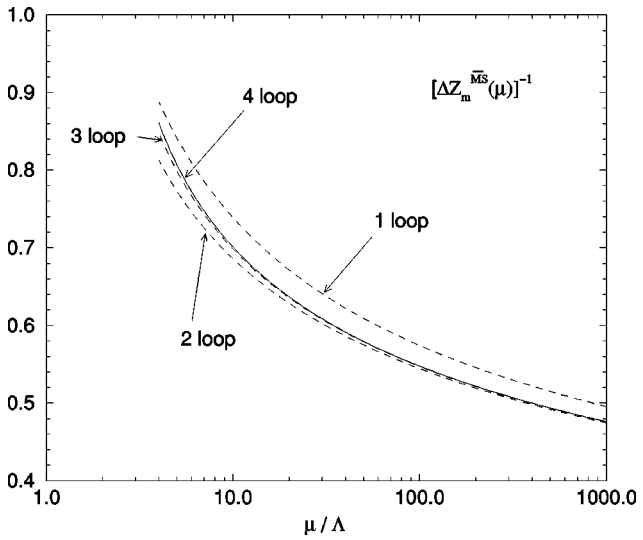

FIG. 1. One-, two-, three-, and four-loop results for $[\Delta Z_m^{\overline{MS}}(\mu)]^{-1}$ in units of $\Lambda^{\overline{MS}}$.

III. DIGRESSION: WHICH SCALE TO USE?

We always need one (or more) experimental numbers as input to set the scale. Ideally, it should not matter what quantity we use. Obvious choices are the force scale r_0 [4], or the string tension $\sqrt{\sigma}$, or some particle mass (e.g., the proton, or for quenched QCD at least, the ρ). So a first requirement is that whatever quantity we use, we should be in a region where the scaling to the continuum limit is the same for all quantities. Thus for r_0 and the string tension we wish that

$$\frac{r_0}{a}(g_0)\times(a\sqrt{\sigma})(g_0)=\text{const} \tag{11}$$

over the $g_0^2\equiv 6/\beta$ region used in the simulations, and indeed for all smaller g_0^2. (We know that this must break down below a value of β around 5.7, due to the appearance of non-universal terms.) In Fig. 2 we show this product. This seems reasonably constant, with a fit value of 1.170(5).

The second requirement is to set the scale in MeV. As we are considering quenched QCD, it is not obvious that choosing scales from different experimental (or phenomenological) quantities will necessarily lead to the same results. Indeed, in the real world [4,10] the values are

$$r_0=0.5\,\text{fm}\equiv(394.6\,\text{MeV})^{-1},$$

$$\sqrt{\sigma}=427\,\text{MeV}, \tag{12}$$

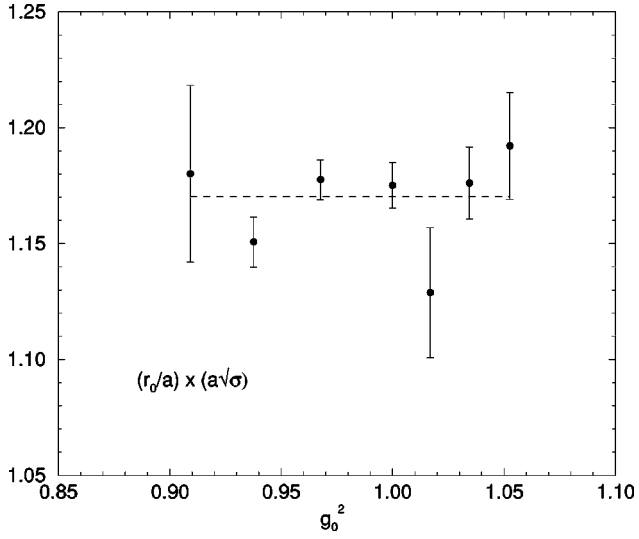

FIG. 2. The product of r_0/a and the string tension $a\sqrt{\sigma}$. $(r_0/a)(g_0)$ is taken from the formula given in [5], while the string tension is taken from [6] ($\beta=5.7$, 5.8, 5.9, 6.4), [7] ($\beta=6.0$, 6.2), [8] ($\beta=6.4$), and [9] ($\beta=6.6$).

($1\ \mathrm{fm}^{-1}=197.3$ MeV) which gives for the product a value of 1.082–almost a 10% difference from the quenched value. As both phenomenological estimates come from the same potential model [11], presumably the quenched lattice potential has a slightly different shape from the continuum potential.

Recently, the ALPHA Collaboration has determined a value for $\Lambda^{\overline{MS}}$ [12] of

$$\Lambda^{\overline{MS}}=0.602(48)/r_0, \tag{13}$$

which may easily be converted using Eq. (11) to the string tension scale. However, the numerical value will then suffer from the same 10% ambiguity. Thus we find

$$\Lambda_{r_0}^{\overline{MS}}=238(19)\ \mathrm{MeV},$$

$$\Lambda_{\sqrt{\sigma}}^{\overline{MS}}=220(18)\ \mathrm{MeV}. \tag{14}$$

Our recent spectrum results [13], using $O(a)$ improved fermions, also show a difference whether one uses the ρ or the proton mass to set the scale. Using r_0 to set the scale is roughly equivalent to using m_ρ.

In the following we shall adopt the r_0 scale as given in [5], namely,

$$\ln(a/r_0)=-1.6805-1.7139(\beta-6)+0.8155(\beta-6)^2-0.6667(\beta-6)^3 \tag{15}$$

(with an error of 0.3% increasing to 0.6% for β in the range $5.7\leqslant\beta\leqslant6.57$), but delay using a numerical value for this scale for as long as possible. For the standard scale of $\mu=2$ GeV this gives, upon solving Eqs. (7) and (9) to the appropriate loop order, the results for $[\Delta Z_m^{\overline{MS}}(\mu)]^{-1}$ shown in Table I. For later reference the results for some other μ values are also given there, together with $\alpha_s^{\overline{MS}}(\mu)$.

IV. DETERMINING THE QUARK MASS

We shall now derive formulas for the quark masses using the conserved vector current (CVC) and the partially conserved axial vector current (PCAC) by assuming Taylor expansions in the bare quark mass for the relevant functions that occur. We distinguish two quark masses. The Ward identities arising from an infinitesimal vector transformation in the partition function lead to a bare quark mass given by

$$am_{q_i}\equiv\frac{1}{2}\left(\frac{1}{\kappa_{q_i}}-\frac{1}{\kappa_c}\right),\quad i=1,2, \tag{16}$$

where κ_{q_i} is the corresponding hopping parameter, and κ_c is the critical hopping parameter. This is the standard definition of the quark mass. Similarly, for an infinitesimal axial transformation the Ward identity (WI) or PCAC definition of the quark mass can be written as

TABLE I. Useful values of $[\Delta Z_m^{\overline{MS}}(\mu)]^{-1}$ and $\alpha_s^{\overline{MS}}(\mu)\equiv[g^{\overline{MS}}(\mu)]^2/4\pi$. The errors are a reflection of the error in Eq. (13). The values of $1/a$ are found from Eq. (15) together with r_0 from Eq. (12).

μ	one-loop	two-loop	three-loop	four-loop
		$[\Delta Z_m^{\overline{MS}}(\mu)]^{-1}$		
2.00 GeV	0.760(10)	0.704(9)	0.718(10)	0.721(10)
2.12 GeV ($1/a$ at $\beta=6.0$)	0.752(10)	0.697(8)	0.711(9)	0.714(10)
2.90 GeV ($1/a$ at $\beta=6.2$)	0.716(8)	0.667(7)	0.677(7)	0.679(8)
3.85 GeV ($1/a$ at $\beta=6.4$)	0.689(7)	0.644(6)	0.652(5)	0.653(6)
		$\alpha_s^{\overline{MS}}(\mu)$		
2.00 GeV	0.268(10)	0.195(6)	0.201(6)	0.202(7)
2.12 GeV ($1/a$ at $\beta=6.0$)	0.261(9)	0.191(5)	0.196(6)	0.197(6)
2.90 GeV ($1/a$ at $\beta=6.2$)	0.228(7)	0.170(5)	0.174(5)	0.175(5)
3.85 GeV ($1/a$ at $\beta=6.4$)	0.205(6)	0.156(3)	0.159(4)	0.159(4)

$$a\tilde{m}_{q_1}+a\tilde{m}_{q_2} \overset{t\gg 0}{=} \frac{\langle \partial_4 \mathcal{A}_4^{q_1q_2}(t)\mathcal{P}^{q_1q_2;smeared}(0)\rangle}{\langle \mathcal{P}^{q_1q_2}(t)\mathcal{P}^{q_1q_2;smeared}(0)\rangle} \tag{17}$$

$$\equiv -\sinh am_{PS}^{q_1q_2}\frac{\langle 0|\hat{\mathcal{A}}_4^{q_1q_2}|PS\rangle}{\langle 0|\hat{\mathcal{P}}^{q_1q_2}|PS\rangle}, \tag{18}$$

where $\mathcal{A}(\mathcal{P})$ is the axial vector current (pseudoscalar density). The precise form of $\mathcal{A}$ and and $\mathcal{P}$ will be given later for the $O(a)$ improved as well as the Wilson cases. We have summed the operators over their spatial planes. While $\mathcal{A}(t)$ and $\mathcal{P}(t)$ should be point operators, to improve the signal $\mathcal{P}(0)$ is smeared over its spatial plane. To obtain the second equation, we have rewritten Eq. (17) in a Fock space and then introduced a complete set of states in the usual way. We have then picked out the lowest pseudoscalar (PS) or 0^{-+} state whose mass we denote by $m_{PS}^{q_1q_2}$.

Both definitions of the quark mass must be renormalized. In a scheme $\mathcal{S}$ at scale M we have

$$m_{q_i}^{\mathcal{S}}(M)=Z_m^{\mathcal{S}}(M,am_{q_i})m_{q_i},$$

$$m_{q_1}^{\mathcal{S}}(M)+m_{q_2}^{\mathcal{S}}(M)=\tilde{Z}_m^{\mathcal{S}}(M,am_{q_1},am_{q_2})(\tilde{m}_{q_1}+\tilde{m}_{q_2}). \tag{19}$$

The Ward identities give $Z_m=1/Z_S$ (from CVC) and $\tilde{Z}_m=Z_A/Z_P$ (from PCAC).

Let us now Taylor expand $\tilde{m}$ and the pseudoscalar mass $m_{PS}^{q_1q_2}$ in terms of the bare quark masses m_{q_i}:

$$\begin{aligned}\tfrac{1}{2}(a\tilde{m}_{q_1}+a\tilde{m}_{q_2})&=\tilde{Y}\Bigg[1+\tilde{c}\tfrac{1}{2}(am_{q_1}+am_{q_2})\\&\quad+\tilde{d}\frac{(am_{q_1})^2+(am_{q_2})^2}{am_{q_1}+am_{q_2}}+\cdots\Bigg]\\&\quad\times\tfrac{1}{2}(am_{q_1}+am_{q_2}),\\(am_{PS}^{q_1q_2})^2&=Y_{PS}\Bigg[1+c_{PS}\tfrac{1}{2}(am_{q_1}+am_{q_2})\\&\quad+d_{PS}\frac{(am_{q_1})^2+(am_{q_2})^2}{am_{q_1}+am_{q_2}}+\cdots\Bigg]\\&\quad\times\tfrac{1}{2}(am_{q_1}+am_{q_2}).\end{aligned} \tag{20}$$

The functions must be symmetric under interchange of the quarks, i.e., $q_1\leftrightarrow q_2$. Only at the lowest (first) order in the quark mass is the functional form simply $am_{q_1}+am_{q_2}$. At the next order both terms, $(am_{q_1}+am_{q_2})^2$ and $(am_{q_1})^2+(am_{q_2})^2$ are allowed. Taylor expanding Eq. (19) and comparing with Eq. (20) gives us

$$\tilde{Y}=\frac{Z_m^{\mathcal{S}}(M)}{\tilde{Z}_m^{\mathcal{S}}(M)}\equiv\frac{Z_P^{\mathcal{S}}(M)}{Z_S^{\mathcal{S}}(M)Z_A}. \tag{21}$$

Renormalization constants which show no explicit quark mass dependence refer to $m_{q_1}=m_{q_2}=0$.

We shall also Taylor expand the matrix elements appearing in Eq. (18). First we define the bare pseudoscalar decay constant by $\langle 0|\hat{\mathcal{A}}_4^{q_1q_2}|PS\rangle=m_{PS}^{q_1q_2}f_{PS}^{q_1q_2}$, and similarly we set $\langle 0|\hat{\mathcal{P}}^{q_1q_2}|PS\rangle=-g_{PS}^{q_1q_2}$. Expanding the decay constants $f_{PS}^{q_1,q_2}$ and $g_{PS}^{q_1q_2}$ to first order in the quark masses gives

$$\tilde{d}=d_{PS}\equiv d, \tag{22}$$

and hence

$$\frac{\frac{1}{2}(a\tilde{m}_{q_1}+a\tilde{m}_{q_2})}{(am_{PS}^{q_1q_2})^2}=\frac{\tilde{Y}}{Y_{PS}}\left[1+\left(\frac{\tilde{c}-c_{PS}}{Y_{PS}}\right)(am_{PS}^{q_1q_2})^2+\cdots\right]. \tag{23}$$

Thus, at least to this order, we have a relation between the WI quark masses and the pseudoscalar mass.

Using Eq. (19) gives the renormalized quark mass, and we additionally use Eq. (8) to rewrite this in a RGI form as

$$\frac{\frac{1}{2}(r_0m_{q_1}^{RGI}+r_0m_{q_2}^{RGI})}{(r_0m_{PS}^{q_1q_2})^2}=c_a^*+c_b^*(r_0m_{PS}^{q_1q_2})^2+\cdots, \tag{24}$$

with

$$c_a^*=\lim_{g_0\to 0}c_a(g_0),\quad c_b^*=\lim_{g_0\to 0}c_b(g_0), \tag{25}$$

and

$$\begin{aligned}c_a&=[\Delta Z_m^{\mathcal{S}}(M)\tilde{Z}_m^{\mathcal{S}}(M)]\times\left[\frac{\tilde{Y}}{Y_{PS}}\right]\times\left(\frac{r_0}{a}\right)^{-1},\\c_b&=[\Delta Z_m^{\mathcal{S}}(M)\tilde{Z}_m^{\mathcal{S}}(M)]\times\left[\frac{\tilde{Y}}{Y_{PS}}\right]\\&\quad\times\left[\frac{-c_{PS}}{Y_{PS}}\left(\frac{r_0}{a}\right)^{-2}\right]\times\left(\frac{r_0}{a}\right)^{-1}.\end{aligned} \tag{26}$$

Upon taking the continuum limit $g_0\to 0$, any scaling violations will show themselves as nonconstant c_a, c_b functions. Equation (24) is the main result of this analysis. Given c_a^*, c_b^* and the pseudoscalar mass, we can then determine the quark masses.

For the $K^+(u\bar{s})$ we set $q_1=u$, $q_2=s$, and for the $K^0(d\bar{s})$ we set $q_1=d$, $q_2=s$. Together with the $\pi^+(u\bar{d})$, with $q_1=u$, $q_2=d$, this gives, from Eq. (24),

$$r_0 m_s^{RGI} = c_a^*[(r_0 m_{K^+})^2 + (r_0 m_{K^0})^2 - (r_0 m_{\pi^+})^2] + c_b^*[(r_0 m_{K^+})^4 + (r_0 m_{K^0})^4 - (r_0 m_{\pi^+})^4] + \cdots,$$

$$r_0 m_l^{RGI} = c_a^*(r_0 m_{\pi^+})^2 + c_b^*(r_0 m_{\pi^+})^4 + \cdots, \quad (27)$$

where we have defined $m_l^{RGI} = (m_u^{RGI} + m_d^{RGI})/2$, i.e., the average of the u/d quarks. We have ignored any small corrections due to electromagnetic effects.

V. NUMERICAL RESULTS

A. Pseudoscalar mesons and bare quark masses

For degenerate quark masses from Eq. (20) we have

$$a\tilde{m}_q = \tilde{Y}[1 + (\tilde{c} + d) a m_q + \cdots] a m_q,$$

$$(a m_{PS})^2 = Y_{PS}[1 + (c_{PS} + d) a m_q + \cdots] a m_q, \quad (28)$$

and

$$\frac{a\tilde{m}_q}{(a m_{PS})^2} = \frac{\tilde{Y}}{Y_{PS}}\left[1 + \left(\frac{\tilde{c} - c_{PS}}{Y_{PS}}\right)(a m_{PS})^2 + \cdots\right], \quad (29)$$

where $m_{PS} \equiv m_{PS}^{qq}$ (i.e., $q_1 = q_2 \equiv q$). Equation (29) gives $\tilde{Y}/Y_{PS}$ for the c_a term in Eq. (27), but the gradient $(\tilde{c} - c_{PS})/Y_{PS}$ is not sufficient to give $-c_{PS}/Y_{PS}$ for the c_b term. For $O(a)$ improved fermions, associating the mass expansion parameters b_A, b_P, and b_m [14] with our expansions, we find $\tilde{c} \equiv -(b_A - b_P)$ and $d \equiv b_m$. First order perturbation theory [15] gives $\tilde{c} \sim 0.001 g_0^2$.[1] On top of that $\tilde{c}/c_{PS} = O(a)$, so that the effect of $\tilde{c}$ can safely be ignored. For Wilson fermions we shall assume that either $\tilde{c}$ is small in comparison with c_{PS}, as above, or that the complete term $c_b (r_0 m_K)^2$ is small when compared with c_a. As we shall see, little error is introduced by this assumption.

We have computed the pseudoscalar mass m_{PS} and the *WI* bare quark mass both, for $O(a)$ improved fermions and Wilson fermions. For improved fermions the calculations were done at $\beta = 6.0, 6.2, 6.4$ and $c_{SW} = 1.769, 1.614, 1.526$ [14], respectively, while for Wilson fermions we only did calculations at $\beta = 6.0, 6.2$. The computational methods used are standard. For the pseudoscalar mass we used the correlation function

$$C(t) = \langle \mathcal{P}^{smeared}(t) \mathcal{P}^{smeared}(0) \rangle \overset{t \gg 0}{=} A[e^{-m_{PS} t} + e^{-m_{PS}(T-t)}], \quad (30)$$

T being the temporal extent of the lattice. To improve the signal, a Jacobi-smeared operator was used, as described in [10]. For Wilson fermions the pseudoscalar meson mass results can also be found in [10]. The $O(a)$ improved results for m_{PS} are given in Table V in the Appendix. The various κ values used, the lattice size, and the number of configurations generated are also collated there.

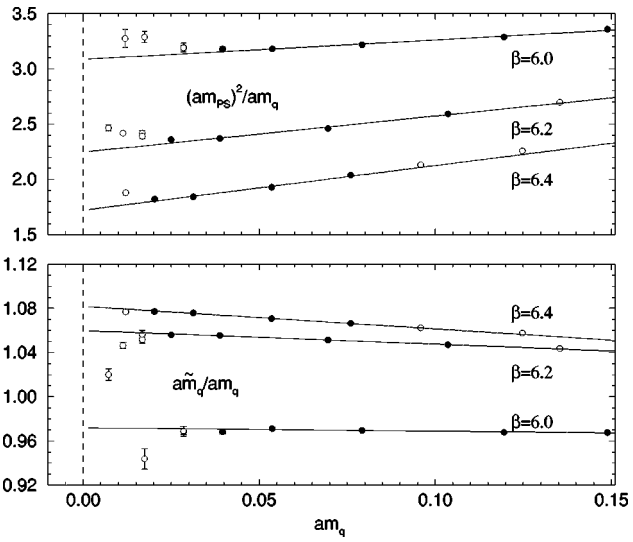

FIG. 3. $(am_{PS})^2/am_q$ and $a\tilde{m}_q/am_q$ against am_q for $O(a)$ improved fermions. Filled circles denote points used in the fits.

For $a\tilde{m}_q$ the ratio of two point correlation functions as given in Eq. (17) was used. For $O(a)$ improved fermions, as well as the action, the operators must also be improved:

$$\mathcal{A}_\mu = A_\mu + c_A a \partial_\mu P, \qquad \mathcal{P} = P, \quad (31)$$

where $A_\mu = \bar{q}\gamma_\mu\gamma_5 q$ and $P = \bar{q}\gamma_5 q$. By choosing the improvement coefficient $c_A(g_0)$ appropriately, the Ward identity can be made exact to $O(a)$. $c_A(g_0)$ is nonperturbatively known [17]. In Table VI in the Appendix we give our results for $a\tilde{m}_q$.

Let us first discuss $O(a)$ improved fermions. In Fig. 3 we show the ratios $(am_{PS})^2/am_q$ and $a\tilde{m}_q/am_q$ against am_q, while in Fig. 4 we plot $a\tilde{m}_q/(am_{PS})^2$ against $((r_0/a) \times (am_{PS}))^2$. We must now search for a region where Eq. (28), without higher order terms, is valid. For large quark mass values we expect nonlinear terms, while for small quark masses quenched QCD chiral logarithms become significant. Finite volume effects do not seem to be a problem, as for $\beta = 6.0$, $\kappa = 0.1342$ and $\beta = 6.2$, $\kappa = 0.1352$ we have made runs on two different volumes, without significant changes in the results.

We now make some cuts. In Fig. 4 we see that for small quark masses there are significant deviations from linearity. In particular the light quark mass m_l lies in a region where no direct linear extrapolation is possible. However, above $m_{PS} \approx \sqrt{2} m_K$ deviations from linearity seem small. For example, adding or removing a point does not change the constant in Eq. (29) at all and the gradient by less than one σ. We shall thus assume that at least above the strange quark mass any effects of chiral logarithms are small. For heavy

[1] A nonperturbative estimate [16], however, gives $\tilde{c} \sim -0.15$ at $\beta = 6.2$.

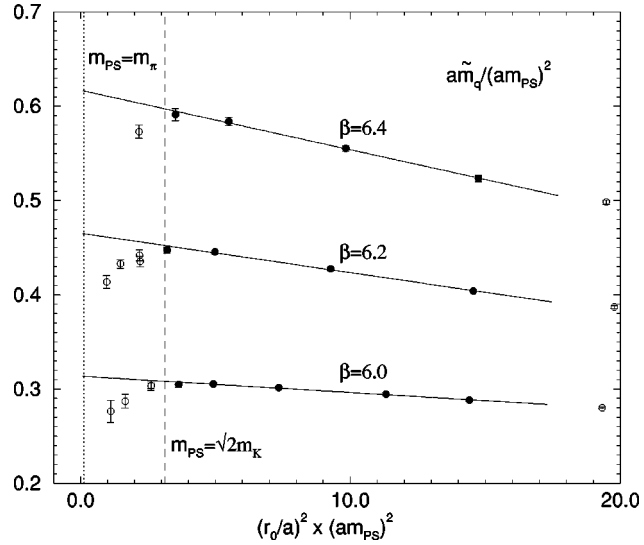

FIG. 4. $a\tilde{m}_q/(am_{PS})^2$ against $[(r_0/a)\times(am_{PS})]^2$ for $O(a)$ improved fermions. Filled circles denote points used in the fits. The dashed line (~ 3.13) is $m_{PS}=\sqrt{2}m_K$ (which here corresponds to a fictitious $s\bar{s}$ bound state) while the dotted line (~ 0.125) is m_π.

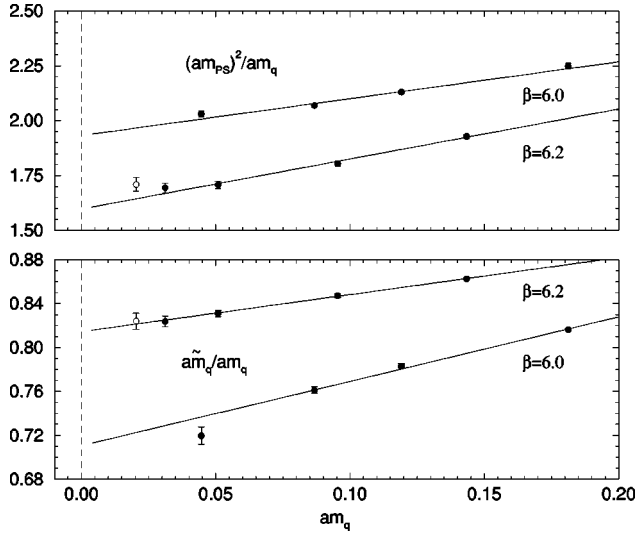

FIG. 5. $(am_{PS})^2/am_q$ and $a\tilde{m}_q/am_q$ against am_q for Wilson fermions.

quark masses, on the other hand, linearity is still present until at least $m_q \approx 3m_s \approx \frac{1}{3}m_c$. [Note that $2(r_0 m_D)^2 \sim 44.9$]. In this interval lie four or more quark masses. The results of the various fits are given in Table II.

For Wilson fermions we simply set $\mathcal{A}_\mu = A_\mu$. The results for $a\tilde{m}_q$ have also been given in [10]. In Figs. 5 and 6 we show the ratios $(am_{PS})^2/am_q$, $a\tilde{m}_q/am_q$, and $a\tilde{m}_q/(am_{PS})^2$. Similar fit ranges as for improved fermions seem appropriate once more.

To illustrate the g_0^2 dependence of some of these results, we show in Fig. 7 the results for $\tilde{Y}$ taken from Table II together with Padé-like interpolations of the form

$$\tilde{Y}(g_0) = \frac{1 + p_1 g_0^2 + p_2 g_0^4}{1 + (p_1 - c) g_0^2 + p_3 g_0^4}, \tag{32}$$

arranged so that the perturbative result $\tilde{Y}(g_0) = 1 + c g_0^2$ with $c = 0.09051$ for improved fermions and 0.05195 for Wilson fermions is obtained for small g_0^2. Possible Padé interpolations are found to be $(p_1, p_2, p_3) = (-1.24, 0.256, 0.347)$ for $O(a)$ improved fermions and $(-0.944, 0.00, 0.0746)$ for Wilson fermions. Also shown for comparison are $O(a)$ improved results found in [16]. We see that for $O(a)$ improved fermions first order perturbation theory is good for $g_0^2 \lesssim 0.96$, while for Wilson fermions a breakdown occurs much earlier.

Thus we now have estimates for $\tilde{Y}/Y_{PS}$ and $(\tilde{c} - c_{PS})/Y_{PS}$. $\tilde{Y}$ will also be needed for Wilson fermions.

TABLE II. Fit values.

β	$\frac{\tilde{Y}}{Y_{PS}}$	$\frac{\tilde{Y}}{Y_{PS}} \times \frac{\tilde{c} - c_{PS}}{Y_{PS}} \left(\frac{r_0}{a}\right)^{-2}$	$\tilde{Y}$
		$O(a)$ improved fermions	
6.0	0.314(2)	−0.0017(2)	0.972(6)
6.2	0.465(2)	−0.0042(2)	1.060(3)
6.4	0.617(5)	−0.0063(5)	1.082(5)
		Wilson fermions	
6.0	0.368(4)	−0.00025(51)	0.711(12)
6.2	0.502(6)	−0.0036(5)	0.814(10)

B. Renormalization

To compute c_a and c_b we must now determine the factor $\Delta Z_m^S(M) Z_m^S(M)$. For $O(a)$ improved fermions this was done by the ALPHA Collaboration [12] using the Schrödinger functional (SF) method. With the notation of Eq. (8) their result can be written as

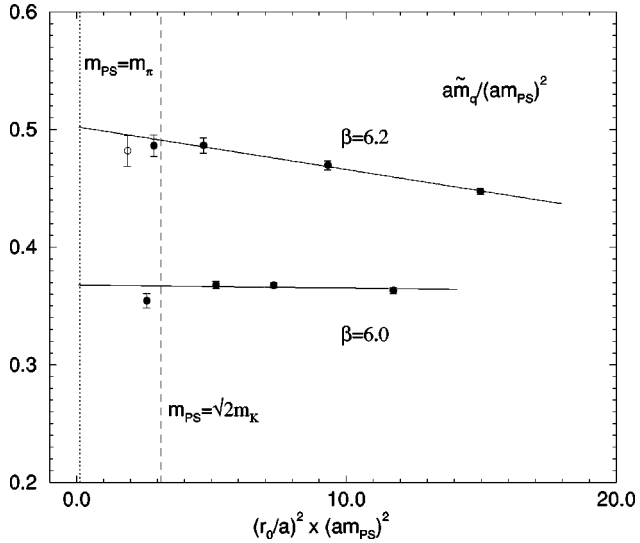

FIG. 6. The same as Fig. 4 but for Wilson fermions.

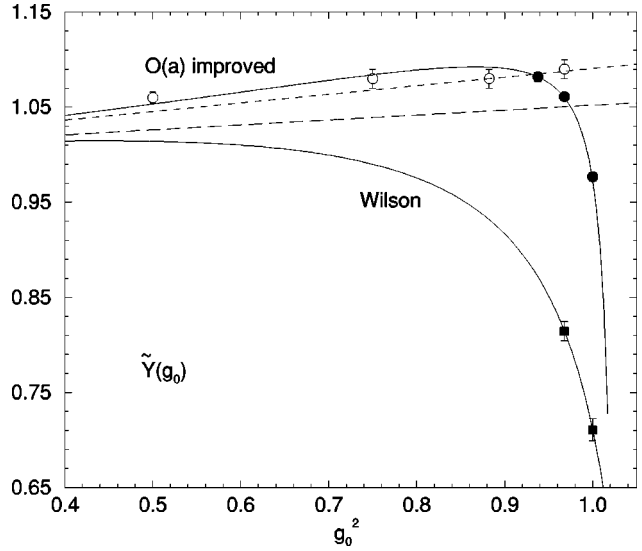

FIG. 7. $\tilde{Y}$ against g_0^2. Our $O(a)$ improved fermion results are shown as filled circles, while those from [16] are shown as open circles. The Wilson fermion results are filled squares. The one-loop perturbation theory results are also shown for the $O(a)$ improved case (dashed line) and the Wilson case (long dashed line).

$$\Delta Z_m^{SF}(L^{-1})\tilde{Z}_m^{SF}(L^{-1}) = 1.752 + 0.321(\beta-6) - 0.220(\beta-6)^2 \quad (33)$$

(valid for $6.0 \leqslant \beta \leqslant 6.5$), where they have worked at a scale given in terms of the box size L. As emphasized previously, this is a mapping from the bare quark mass to the RGI mass, so this function is the same in all schemes. In Eq. (33) the total error is about 2%.

For Wilson fermions we use the method proposed in [18] and refined in [19]. This mimics perturbation theory in a certain momentum subtraction (MOM) scheme by considering amputated quark Green's functions in, say, the Landau gauge, with an appropriate operator insertion. The renormalization constant is fixed at some scale p^2. This gives a nonperturbative determination of $Z_S^{MOM}(p)$. [$Z_P^{MOM}(p)$ is not suitable, as chiral symmetry breaking means that $Z_P^{MOM} \to 0$ as we approach the chiral limit, as recently emphasized in [20].] More details of the method, our momentum source approach, and results are given in [19]. As $\Delta Z_m^{\overline{MS}}$ is known in the $\overline{\text{MS}}$ scheme at scale μ (see Fig. 1 and Table I), we can write

$$\Delta Z_m^{MOM}(p)\tilde{Z}_m^{MOM}(p) = \frac{\Delta Z_m^{\overline{MS}}(\mu)}{Z_S^{\overline{MS}}(\mu)\tilde{Y}} \equiv F(\beta), \quad (34)$$

where we have used Eq. (21) and the definitions $Z_m = 1/Z_S$, $\Delta Z_m = 1/\Delta Z_S$ and

$$Z_S^{\overline{MS}}(\mu) = X_{S;MOM}^{\overline{MS}}(\mu,p) Z_S^{MOM}(p), \quad (35)$$

with

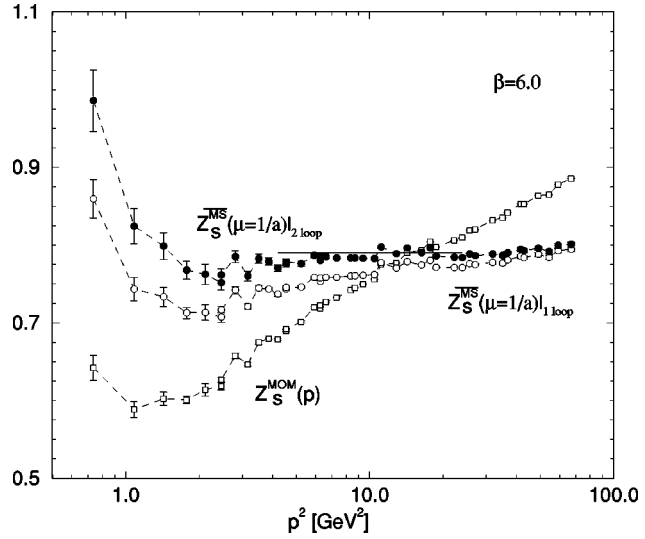

FIG. 8. $Z_S^{\overline{MS}}(\mu=1/a)$ against p^2 for $\beta=6.0$. (See [19] for details.) The open squares are the original data, in the chiral limit, while the filled circles represent the results of multiplying $Z^{MOM}(p)$ by X using both coefficients B_1 and B_2. The open circles are the result of using only the B_1 coefficient. The straight line is a fit to the plateau, the length denoting the fit range chosen.

$$X_{S;MOM}^{\overline{MS}}(\mu,p) = \frac{\Delta Z_S^{MOM}(p)}{\Delta Z_S^{\overline{MS}}(\mu)}. \quad (36)$$

Here X converts the renormalization constant from the MOM scheme to the $\overline{\text{MS}}$ scheme and can be calculated using a continuum regularization (e.g., naive dimensional regularization). So we can write

$$X_{S;MOM}^{\overline{MS}}(\mu,\mu) = \frac{Z_S^{\overline{MS}}(\mu)}{Z_S^{MOM}(\mu)} = 1 + \frac{\alpha_s^{\overline{MS}}(\mu)}{4\pi} B_1 + \left(\frac{\alpha_s^{\overline{MS}}(\mu)}{4\pi}\right)^2 B_2 + \cdots, \quad (37)$$

with $B_1 = 16/3$ [10]. The coefficient B_2 has recently been calculated [21], giving in the Landau gauge for $N_f = 0$ flavors a value of 177.48452. Hence, knowing the coefficients B_1, B_2, we can trace back to the more general expression for X. A suitable formula is

TABLE III. Fit values for the Wilson renormalization constants.

β	$Z_S^{\overline{MS}}(\mu=1/a)$	$\Delta Z_m^{MOM}(p)\tilde{Z}_m^{MOM}(p)$
6.0	0.790(5)	2.49(6)
6.2	0.803(5)	2.25(4)

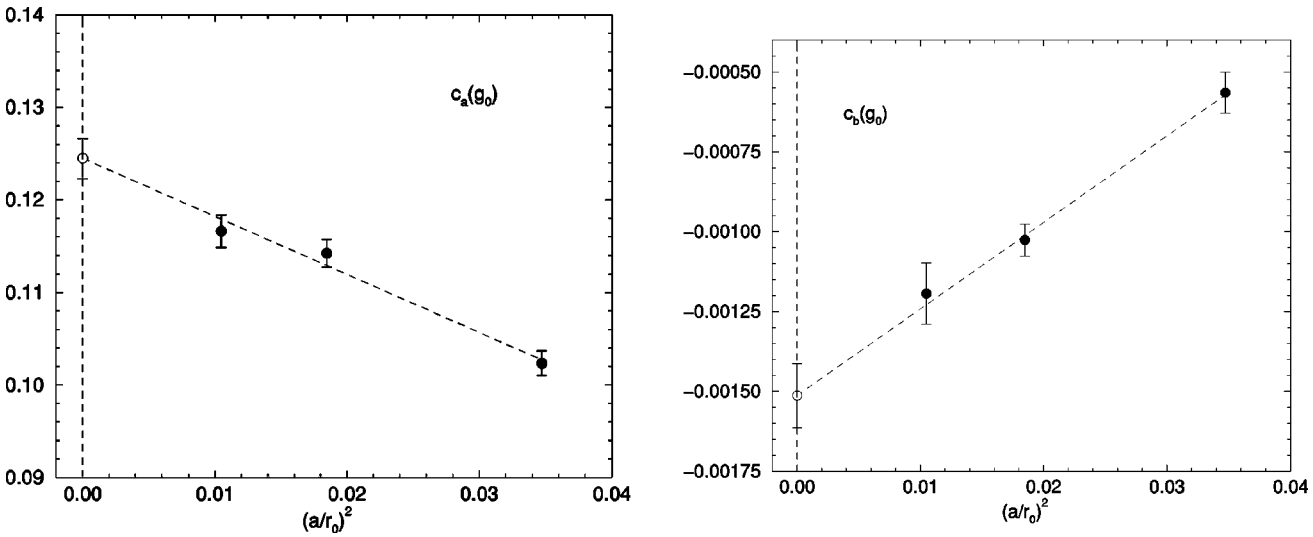

FIG. 9. The continuum extrapolation for c_a and c_b for $O(a)$ improved fermions.

$$[X^{\overline{MS}}_{S;MOM}(\mu,p)]^{-1} = \exp\left[\int_{g^{\overline{MS}}(p)}^{g^{\overline{MS}}(\mu)} d\xi \frac{\gamma_m^{\overline{MS}}(\xi)}{\beta^{\overline{MS}}(\xi)} + \int_0^{g^{\overline{MS}}(p)} d\xi \left(\frac{\gamma_m^{\overline{MS}}(\xi) - \gamma_m^{MOM}(G(\xi))}{\beta^{\overline{MS}}(\xi)}\right)\right] \tag{38}$$

[$g^{MOM} = G(g^{\overline{MS}})$ from Eq. (10)]. Armed with this estimate for X, then from Eq. (35) we see that $Z_S^{\overline{MS}}(\mu)$ should be independent of p^2, so plotting $Z_S^{\overline{MS}}(\mu)$ against p^2 we expect to see a plateau. In Fig. 8 we show this, plotting first the original data, extrapolated to the chiral limit, then the results for $Z_S^{\overline{MS}}$ when only using B_1, and finally using both B_1 and B_2. We see the data for Z_S becoming flatter. The results of the fit are given in the first column of Table III. The appropriate values for $\tilde{Y}$ (see Table II) and $\Delta Z_m^{\overline{MS}}(\mu = 1/a)$ (see Table I) are substituted in Eq. (34) to give the results listed in the second column of this table.

VI. CONTINUUM RESULTS

Plotting c_a and c_b against a^2 for $O(a)$ improved fermions, and against a for Wilson fermions, we can now extrapolate these coefficients to the continuum limit. In Fig. 9 we show the results for c_a and c_b for improved fermions. A linear fit is also plotted. The results of this fit are given in Table IV. As anticipated, using the first order perturbative result from [15] for $\tilde{c}$ in c_b has no influence on the result.[2] In Fig. 10 we show the equivalent results for Wilson fermions. In this case, as we only have two β values, the fit degenerates to an extrapolation. The results of this extrapolation are also given in Table IV. We note that the results for $O(a)$ improved fermions and Wilson fermions for c_a^* are compatible with each other. Upon inserting these numbers in Eq. (27), we find our estimate for the RGI strange and u/d quark masses. To convert to physical numbers, we now have in quenched QCD the uncertainty in the scale, as discussed in Sec. III. If we use the scale $r_0 = 0.5$ fm, Eq. (12), then together with the experimental values of the π and K masses, namely $m_{\pi^+} = 139.6$ MeV and $m_{K^+} = 493.7$ MeV, $m_{K^0} = 497.7$ MeV, we find the results for $O(a)$ improved fermions

$$m_s^{RGI} = 146(4)\ \text{MeV},$$
$$m_l^{RGI} = 6.1(2)\ \text{MeV}. \tag{39}$$

TABLE IV. The continuum extrapolation of $c_a \to c_a^*$ and $c_b \to c_b^*$ for $O(a)$ improved fermions and Wilson fermions. The errors are statistical.

c_a	$\beta = 6.0$	$\beta = 6.2$	$\beta = 6.4$	c_a^*
$O(a)$ improved	0.1023(13)	0.1142(15)	0.1166(18)	0.124(2)
Wilson	0.1709(43)	0.1537(34)	–	0.107(17)
c_b	$\beta = 6.0$	$\beta = 6.2$	$\beta = 6.4$	c_b^*
$O(a)$ improved	−0.000565(64)	−0.00103(4)	−0.00119(10)	−0.0015(1)
Wilson	−0.00012(24)	−0.00111(15)	–	−0.0038(9)

[2]Note, however, that the nonperturbative estimate from [16] at $\beta = 6.2$ is $\tilde{c}/Y_{PS} \times (r_0/a)^{-2} \sim -0.0012$ and has a similar order of magnitude to the kept term.

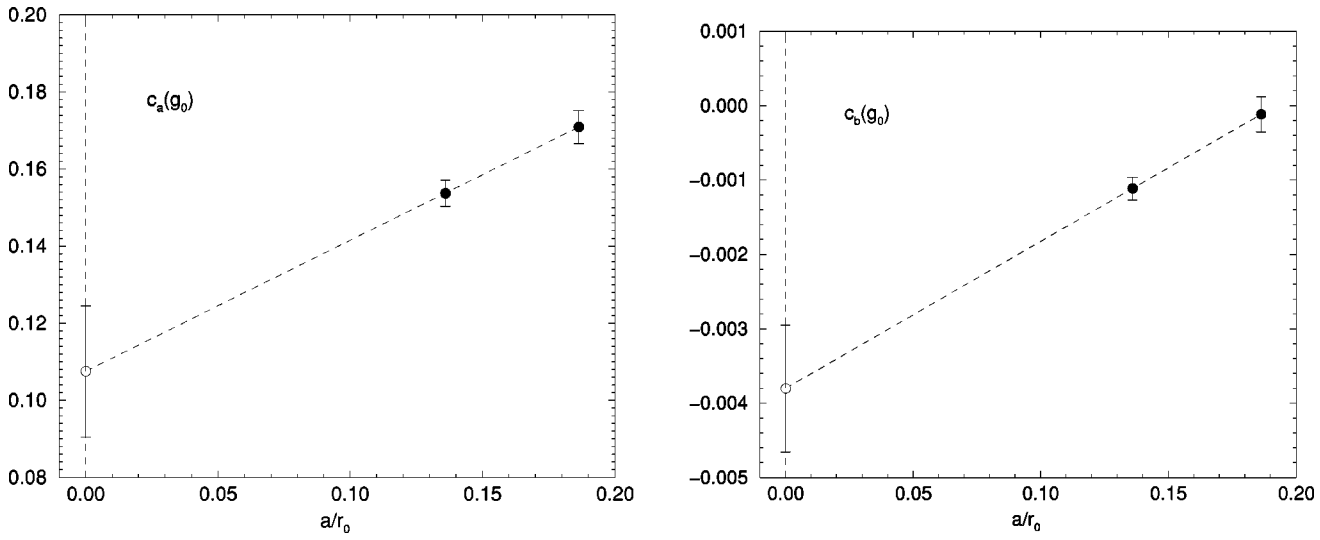

FIG. 10. The continuum extrapolation for c_a and c_b for Wilson fermions.

The error comes from Table IV and from Eq. (33). As can also be seen from Table IV, most of the result comes from the constant term, with the slope giving only a small correction to the answer.

For Wilson fermions we have $m_s^{RGI}=121(20)$ MeV, $m_l^{RGI}=5.3(8)$ MeV. This result is somewhat lower than the $O(a)$ improved numbers. We ascribe this mainly to the fact that we only have two values of β, which makes a continuum extrapolation more difficult. Also the number of κ values used and the size of the data sets are smaller than for $O(a)$ improved fermions. Nevertheless, within a one-standard deviation the results are in agreement.

In the $\overline{\text{MS}}$ scheme at the ''standard'' value of $\mu=2$ GeV, using the four-loop results from Table I, we find for $O(a)$ improved fermions

$$m_s^{\overline{MS}}(\mu=2\ \text{GeV})=105(4)\ \text{MeV},$$

$$m_l^{\overline{MS}}(\mu=2\ \text{GeV})=4.4(2)\ \text{MeV}. \tag{40}$$

The corresponding Wilson results are $m_s^{\overline{MS}}(\mu=2\ \text{GeV})=87(15)$ MeV and $m_l^{\overline{MS}}(\mu=2\ \text{GeV})=3.8(6)$ MeV.

Note that for the m_l quark mass result we have simply extrapolated the fits for the strange quark mass result downwards. The mass ratio m_s/m_l for $O(a)$ improved fermions is ≈ 23.9, which is very close to the value given in leading order chiral perturbation theory—namely $(m_{K^+}^2+m_{K^0}^2-m_{\pi^+}^2)/m_{\pi^+}^2\approx 24.2$ [see Eq. (27)]. This is simply because $|c_b^*|\ll|c_a^*|/(r_0 m_K)^2$, and so the second term in Eq. (27) is almost negligible. The mass ratio is then independent of c_a^*.

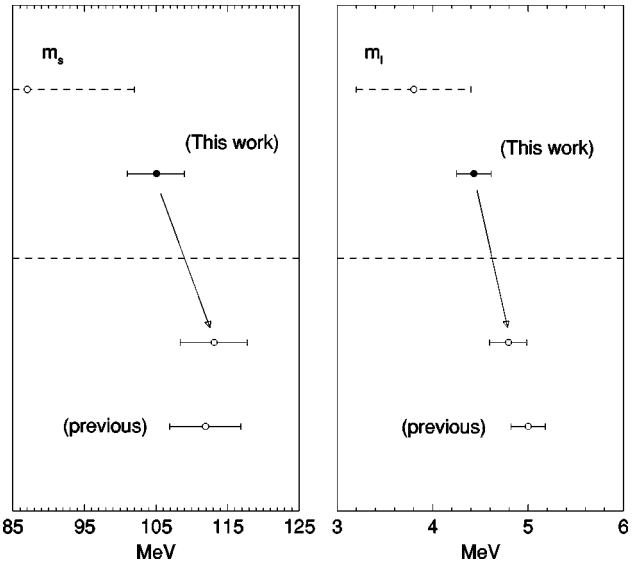

FIG. 11. The strange and light quark masses from Eq. (40) (''this work''). The Wilson fermion results are shown dotted. Also shown is our previous result (''previous'') [10]. The arrows denote the result when using $\sqrt{\sigma}$ as a scale.

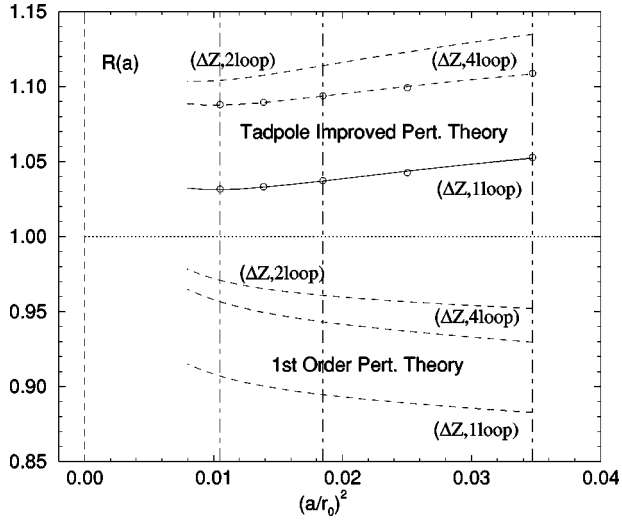

FIG. 12. The results for the ratio R as defined in Eq. (43). $Z_m^{\overline{MS}}$ has been determined from Eq. (41) or Eq. (42) and $\Delta Z_m^{\overline{MS}}$ taken from Table I. A simple interpolation has been used between the β values. The dot-dashed vertical lines correspond to $\beta=6.0$, 6.2, 6.4, from right to left.

TABLE V. Parameter values used in the simulations, together with the measured pseudoscalar mass.

β	c_{sw}	κ	Volume	No. configs.	am_{PS}
6.0	1.769	0.1217	$16^3\times32$	$O(150)$	1.2546(12)
6.0	1.769	0.1263	$16^3\times32$	$O(150)$	0.9704(11)
6.0	1.769	0.1285	$16^3\times32$	$O(150)$	0.8189(11)
6.0	1.769	0.1300	$16^3\times32$	$O(160)$	0.7071(16)
6.0	1.769	0.1310	$16^3\times32$	$O(160)$	0.6268(16)
6.0	1.769	0.1324	$16^3\times32$	$O(990)$	0.5042(7)
6.0	1.769	0.1333	$16^3\times32$	$O(990)$	0.4122(9)
6.0	1.769	0.1338	$16^3\times32$	$O(520)$	0.3549(12)
6.0	1.769	0.1342	$16^3\times32$	$O(1300)$	0.3012(10)
6.0	1.769	0.1342	$24^3\times32$	$O(200)$	0.3017(13)
6.0	1.769	0.1346	$24^3\times32$	$O(200)$	0.2390(12)
6.0	1.769	0.1348	$24^3\times32$	$O(200)$	0.1978(16)
6.2	1.614	0.1247	$24^3\times48$	$O(100)$	1.0284(9)
6.2	1.614	0.1294	$24^3\times48$	$O(100)$	0.7217(9)
6.2	1.614	0.1310	$24^3\times48$	$O(100)$	0.6043(9)
6.2	1.614	0.1321	$24^3\times48$	$O(260)$	0.5183(6)
6.2	1.614	0.1333	$24^3\times48$	$O(560)$	0.4136(6)
6.2	1.614	0.1344	$24^3\times48$	$O(560)$	0.3034(6)
6.2	1.614	0.1349	$24^3\times48$	$O(560)$	0.2431(7)
6.2	1.614	0.1352	$24^3\times48$	$O(260)$	0.2016(10)
6.2	1.614	0.1352	$32^3\times64$	$O(110)$	0.2005(9)
6.2	1.614	0.1354	$32^3\times64$	$O(290)$	0.1657(6)
6.2	1.614	0.13555	$32^3\times64$	$O(280)$	0.1339(7)
6.4	1.526	0.1313	$32^3\times48$	$O(100)$	0.5305(9)
6.4	1.526	0.1323	$32^3\times48$	$O(100)$	0.4522(10)
6.4	1.526	0.1330	$32^3\times48$	$O(100)$	0.3935(12)
6.4	1.526	0.1338	$32^3\times48$	$O(200)$	0.3213(8)
6.4	1.526	0.1346	$32^3\times48$	$O(200)$	0.2402(8)
6.4	1.526	0.1350	$32^3\times48$	$O(200)$	0.1923(9)
6.4	1.526	0.1353	$32^3\times64$	$O(260)$	0.1507(8)

TABLE VI. Results for the Ward identity quark mass $2a\tilde{m}_q$.

β	c_{sw}	κ	$2a\tilde{m}_q^{(0)}$	$2a\tilde{m}_q^{(1)}$	$2a\tilde{m}_q$
6.0	1.769	0.1217	0.9677(7)	1.7867(33)	0.8197(5)
6.0	1.769	0.1263	0.5936(4)	1.0173(24)	0.5093(3)
6.0	1.769	0.1285	0.4340(3)	0.7080(22)	0.3754(3)
6.0	1.769	0.1300	0.3314(3)	0.5227(21)	0.2881(3)
6.0	1.769	0.1310	0.2651(3)	0.4072(20)	0.2313(3)
6.0	1.769	0.1324	0.1751(1)	0.2609(8)	0.1535(1)
6.0	1.769	0.1333	0.1186(1)	0.1737(7)	0.1042(1)
6.0	1.769	0.1338	0.08734(21)	0.1274(9)	0.07678(18)
6.0	1.769	0.1342	0.06282(16)	0.09217(62)	0.05519(15)
6.0	1.769	0.1342	0.06294(27)	0.0932(12)	0.05522(25)
6.0	1.769	0.1346	0.03772(32)	0.0584(11)	0.03289(32)
6.0	1.769	0.1348	0.02485(37)	0.0399(12)	0.02154(37)
6.2	1.614	0.1247	0.7342(3)	1.1520(18)	0.6915(2)
6.2	1.614	0.1294	0.4011(2)	0.5451(12)	0.3809(2)
6.2	1.614	0.1310	0.2966(2)	0.3776(10)	0.2826(2)
6.2	1.614	0.1321	0.2272(1)	0.2748(7)	0.2170(1)
6.2	1.614	0.1333	0.15265(5)	0.1741(4)	0.14620(5)
6.2	1.614	0.1344	0.08542(6)	0.09336(36)	0.08196(5)
6.2	1.614	0.1349	0.05510(6)	0.05985(34)	0.05288(6)
6.2	1.614	0.1352	0.03688(11)	0.04073(46)	0.03537(11)
6.2	1.614	0.1352	0.03703(12)	0.04046(37)	0.03553(12)
6.2	1.614	0.1354	0.02478(6)	0.02773(18)	0.02375(6)
6.2	1.614	0.13555	0.01549(8)	0.01802(20)	0.01482(8)
6.4	1.526	0.1313	0.2709(1)	0.2870(9)	0.2637(1)
6.4	1.526	0.1323	0.2090(1)	0.2074(9)	0.2038(1)
6.4	1.526	0.1330	0.1660(1)	0.1567(8)	0.1621(1)
6.4	1.526	0.1338	0.1172(1)	0.1045(4)	0.11461(6)
6.4	1.526	0.1346	0.06882(6)	0.05799(38)	0.06736(6)
6.4	1.526	0.1350	0.04467(7)	0.03739(35)	0.04373(6)
6.4	1.526	0.1353	0.02661(5)	0.02276(22)	0.02603(5)

In Fig. 11 we plot our results. Below the dotted line, we have given our previous result [10], using the string tension as the scale, as given in Eq. (12). As a comparison we have also replotted our result given in Eq. (40) using $\sqrt{\sigma}$ as the scale. A reasonable agreement is seen. As our previous result used tadpole improved (TI) perturbation theory to determine the renormalization constant, it would seem that the use of TI perturbation theory does not introduce much error. In the next section we shall briefly investigate this point.

VII. DIGRESSION: COMPARISON WITH TADPOLE-IMPROVED PERTURBATION THEORY

In this section we shall discuss how reliable TI perturbation theory is. Lowest order perturbation theory gives

$$Z_S^{\overline{MS}}(\mu=1/a)=1-\frac{g_0^2}{16\pi^2}C_F B^{\overline{MS}}(c_{SW})+O(g_0^4). \quad (41)$$

The B coefficient is uncomfortably large [10]. In [22] this was traced to large tadpole diagrams in the perturbation expansion and also to the expansion in a nonphysical (bare) coupling constant. Removing the tapole diagrams and expanding in (say) $\alpha_s^{\overline{MS}}$ gives the improved series

$$Z_S^{\overline{MS}}(\mu=1/a)=u_0\left(1-\frac{\alpha_s^{\overline{MS}}(\mu=1/a)}{4\pi}C_F[B^{\overline{MS}}(\tilde{c}_{SW})-\pi^2]\right)+O(\alpha_s^2), \quad (42)$$

with $u_0=\langle\frac{1}{3}\mathrm{Tr}\,U_{plaq}\rangle^{1/4}$ to be numerically determined, and $\tilde{c}_{SW}=c_{SW}u_0^3$. A description of our variation of this procedure is given in [10]. In particular, we choose c_{SW} to be the nonperturbatively determined result, rather than setting it to be equal to $1/u_0^3$. $\alpha_s^{\overline{MS}}$ corresponds to the four-loop results (see Table I) also used in [22].

As we now have a genuine nonperturbative determination of Z_m available, it is of interest to compare how the different results scale to the continuum limit. It is convenient to first define for two $O(a)$ improved estimations of the renormalization constant the ratio

$$R=\frac{\Delta Z_m^{\mathcal{S}_1}(M_1)Z_m^{\mathcal{S}_1}(M_1)}{\Delta Z_m^{\mathcal{S}_2}(M_2)Z_m^{\mathcal{S}_2}(M_2)}=1+O(a^2). \tag{43}$$

For $\mathcal{S}_2$ we choose the *SF* scheme and the result given in Eq. (33), while for $\mathcal{S}_1$ we use the $\overline{\text{MS}}$ scheme, together with either the perturbative result, Eq. (41), or the TI result, Eq. (42).

In Fig. 12 we show the results for the ratio R for perturbation theory and TI perturbation theory, using consistently the one-, two-, and four-loop results from Table I. As we originally used one-loop perturbation theory results, it seems more consistent to also use the one-loop result for ΔZ_m when converting $Z_S^{\overline{MS}}$ to the RGI result. This gives the solid line in the figure. This was the approach adopted in [10]. We expect $O(a)$ effects to become apparent as $a^2\to 0$ if $\mathcal{S}_1$ is not exactly $O(a)$ improved. However, a linear fit in a^2 for the TI result (with one-loop ΔZ_m) appears to go to $R=1$ with an error of only about 2%, while for the equivalent perturbative result the error is about 10%. Thus, in this case tadpole improving the perturbative result does give better results. However, choosing other loop orders changes the picture somewhat and can make using perturbation theory a better choice. We would like to emphasize that this picture does not have to hold for other renormalization constants. Strictly speaking a case-by-case analysis is required.

VIII. CONCLUSIONS

In this article we have calculated the strange and u/d quark masses for quenched QCD, both for $O(a)$ improved fermions and Wilson fermions, using a nonperturbatively determined renormalization constant. Our results are given in Eq. (40) and the lines that follow it. Corrections to leading order chiral perturbation theory are small, if we stay away from the region where chiral logarithms become significant. We have also seen that using TI perturbation theory rather than simple perturbation theory does not automatically lead to an improvement of the continuum result.

Note added. While this work was being completed, we received a copy of [23]. This contains some similar results to ours.

ACKNOWLEDGMENTS

The numerical calculations were performed on the Quadrics *QH2* at NIC (Zeuthen) as well as the Cray *T3E* at ZIB (Berlin) and the Cray *T3E* at NIC (Jülich). We wish to thank all institutions for their support.

APPENDIX

In Table V we give our parameter values used in the $O(a)$ improved fermion simulations together with the measured pseudoscalar mass. For most of the overlapping values with [10] there has been some increase in statistics. The results for the WI quark mass, $a\tilde{m}_q$, are first split into two pieces. $2a\tilde{m}_q^{(0)}$ denotes the mass coming from the $\langle\partial_4 A_4 P^{smeared}\rangle/\langle PP^{smeared}\rangle$ ratio, while $2a\tilde{m}_q^{(1)}$ is the result of $\langle\nabla_4^2 PP^{smeared}\rangle/\langle PP^{smeared}\rangle$. The sum $2a\tilde{m}_q=2a\tilde{m}_q^{(0)}+2c_A a\tilde{m}_q^{(1)}$ gives the WI quark mass. All these results are given in Table VI. We define $(\partial_4)_{xy}\equiv(\delta_{x+\hat{4},y}-\delta_{x-\hat{4},y})/2$. $\partial_4\partial_4$ has been replaced by $(\nabla_4^2)_{x,y}\equiv\delta_{x+\hat{4},y}-2\delta_{x,y}+\delta_{x-\hat{4},y}$. In the continuum limit both $\partial_4\partial_4$ and ∇_4^2 give the same derivative. On the lattice we choose the discretization ∇_4^2 with the smallest (temporal) extension. In [10] the choice $\partial_4\partial_4$ was used.

[1] Particle Data Group, C. Caso *et al.*, Eur. Phys. J. C **3**, 1 (1998).
[2] T. van Ritbergen, J. A. M. Vermaseren, and S. A. Larin, Phys. Lett. B **400**, 379 (1997).
[3] J. A. M. Vermaseren, S. A. Larin, and T. van Ritbergen, Phys. Lett. B **405**, 327 (1997).
[4] R. Sommer, Nucl. Phys. **B411**, 839 (1994).
[5] M. Guagnelli, R. Sommer, and H. Wittig, Nucl. Phys. **B535**, 389 (1998).
[6] G. S. Bali and K. Schilling, Int. J. Mod. Phys. C **4**, 1167 (1993).
[7] G. S. Bali, K. Schilling, and A. Wachter, Phys. Rev. D **56**, 2566 (1997).
[8] G. S. Bali and K. Schilling, Phys. Rev. D **47**, 661 (1993).
[9] G. S. Bali (private communication).
[10] M. Göckeler, R. Horsley, H. Perlt, P. Rakow, G. Schierholz, A. Schiller, and P. Stephenson, Phys. Rev. D **57**, 5562 (1998).
[11] E. Eichten, K. Gottfried, T. Kinoshita, K. D. Lane, and T. M. Yan, Phys. Rev. D **21**, 203 (1980).
[12] S. Capitani, M. Lüscher, R. Sommer, and H. Wittig, Nucl. Phys. **B544**, 669 (1999).
[13] M. Göckeler, R. Horsley, D. Petters, D. Pleiter, P. E. L. Rakow, G. Schierholz, and P. Stephenson, Nucl. Phys. B (Proc. Suppl.) **83–84**, 203 (2000).
[14] M. Lüscher, S. Sint, R. Sommer, and P. Weisz, Nucl. Phys. **B478**, 365 (1996).
[15] S. Sint and P. Weisz, Nucl. Phys. **B502**, 251 (1997).
[16] G. M. de Divitiis and R. Petronzio, Phys. Lett. B **419**, 311 (1998).
[17] M. Lüscher, S. Sint, R. Sommer, P. Weisz, and U. Wolff, Nucl. Phys. **B491**, 323 (1997).
[18] G. Martinelli, C. Pittori, C. T. Sachrajda, M. Testa, and A. Vladikas, Nucl. Phys. **B445**, 81 (1995).
[19] M. Göckeler, R. Horsley, H. Oelrich, H. Perlt, D. Petters, P. E. L. Rakow, A. Schäfer, G. Schierholz, and A. Schiller, Nucl.Phys. **B544**, 699 (1999).
[20] J. Cudell, A. Le Yaouanc, and C. Pittori, Phys. Lett. B **454**, 105 (1999).
[21] E. Franco and V. Lubicz, Nucl. Phys. **B531**, 641 (1998).
[22] G. P. Lepage and P. B. Mackenzie, Phys. Rev. D **48**, 2250 (1993).
[23] J. Garden, J. Heitger, R. Sommer, and H. Wittig, Nucl. Phys. **B571**, 237 (2000).